Electron-capture collisions at keV energies of boron and other multiply charged ions with atoms and molecules. I. Ar, H_2, and He

L. D. Gardner* and J. E. Bayfield†
Department of Physics, Yale University, New Haven, Connecticut 06520
and Department of Physics and Astronomy, University of Pittsburgh, Pittsburgh, Pennsylvania 15260

P. M. Koch
Department of Physics, Yale University, New Haven, Connecticut 06520

I. A. Sellin, D. J. Pegg, and R. S. Peterson‡
Department of Physics and Astronomy, University of Tennessee, Knoxville, Tennessee 37916

M. L. Mallory§ and D. H. Crandall
Oak Ridge National Laboratory, Oak Ridge, Tennessee 37830
(Received 13 September 1978; revised manuscript received 23 April 1979)

Single-electron-capture cross sections have been measured for boron ions B^{q+} with initial charges $q = 2$, 3, and 4 incident on helium, molecular hydrogen, and argon gas targets. The cross sections show little dependence on the incident ion energy for the range studied, $6q$–$23q$ keV. Also reported are double-electron-capture cross sections for B^{3+} incident on H_2 and Ar and for B^{4+} incident on He, H_2, and Ar, as well as a survey of single-electron-capture cross sections for ions of carbon ($2 \leq q \leq 4$), nitrogen ($2 \leq q \leq 5$), and oxygen $2 \leq q \leq 6$) at the single energies $8q$ keV incident on He and Ar targets. In general, it is found that the cross sections do not vary monotonically with the initial charge state, for a fixed colliding atomic species. Each reaction depends in detail on the level structures of both the incident ion and the target atom or molecule.

I. INTRODUCTION

The study of electron capture by multiply charged ions during collisions with atoms or molecules has grown tremendously in the last few years, primarily because it has been recognized that in such collisions the electron is most likely captured into an excited state,[1] which may then decay via photon emission, and also because the cross sections for such processes may be quite large. It is evident, therefore, that electron capture may play an important role in the behavior of high-temperature plasmas as an energy-loss mechanism[2,3] and may also be a technologically feasible means of producing population inversions for x-ray lasers.[4,5] Electron capture has a direct influence on the heating of plasma by injection of neutral beams, which is of immediate interest in the fusion energy program.[6,7]

It has also been recognized recently that electron capture may be the dominant mechanism governing the loss of certain multiply charged ion species observed in the interstellar medium.[8,9] This has had a rather dramatic effect on the choice of theoretical models used indirectly to infer the cosmic x-ray and high-energy-particle fluxes in the interstellar medium; prior to this discovery it had been assumed that radiative recombination was the dominant loss mechanism for these ions.

In 1956 Hasted and Smith[10] reported the first experimental determination of cross sections for electron capture by a multicharged slow ion (i.e., one with a velocity v small compared to v_0, the characteristic velocity of the electron in the hydrogen ground state). Since then Hasted and coworkers[11] have carried out much additional work generally limited to ions with $q \leq 3$ and kinetic energies below those of the present work. In the 1960s Fite *et al.*[12] studied electron-capture collisions of He^{2+} with certain target gases including atomic hydrogen. Shah and Gilbody[13] and Bayfield and Khayrallah[14] have reported additional experimental studies with He^{2+} ions. Experiments were performed in the late 1960s and early 1970s by Zwally and Koopman[15] on the C^{4+} + Arand C^{4+} + He systems and by Zwally and Cable[16] on the B^{3+} + He system. Work has been done on Ar^{8+} + Ar collision systems by Klinger *et al.*[17] Work has been performed very recently by Crandall *et al.*[18] for ions of carbon, nitrogen, and oxygen with charges greater than 3 incident on H_2, and by Crandall[19] on the heliumlike ions of boron, carbon, nitrogen, and oxygen incident on He. Last year Nutt *et al.* reported results for C^{2+} and Ti^{2+} on H_2 (Ref. 44).

The primary purpose of this paper is to report experimental values for the single-electron-capture cross sections for B^{q+} ions, $2 \leq q \leq 4$, at laboratory kinetic energies in the range $0.55q$–$2.1q$ keV/amu incident on the gases H_2, He, and Ar. With the single exception of B^{3+} + He (Ref. 16,

 © 1979 The American Physical Society

19), these collision systems had not been studied previously. Also reported are capture cross sections for C^{q+} $(2 \leq q \leq 4)$, N^{q+} $(2 \leq q \leq 5)$, and O^{q+} $(2 \leq q \leq 6)$ ions at the single energies $8q$ keV incident on He and Ar. Double-electron-capture cross sections for B^{3+} and B^{4+} are also reported here. Attempts will be made in Sec. V of this paper to correlate the observed trends in the measured cross sections with trends in the energy-level structures of the initial and final collision partners. Studies involving these same ions incident on atomic hydrogen will be described in a subsequent article.

II. THEORETICAL BACKGROUND

Atomic collisions with relative velocities $v < v_0$ are often treated within an impact-parameter formalism with the internuclear motion assumed to follow some well-defined trajectory (often a straight line). The two colliding atoms are viewed as forming a transient quasimolecule with well-defined electronic eigenstates and corresponding eigenenergies for each value of the internuclear separation R. The eigenenergies are therefore parametric functions of R and are usually called "potential-energy curves." Transitions of the system from one potential-energy curve to another (i.e., transitions between the system's eigenstates) may be induced not only by the "perturbation" caused by the nuclear motion but also by any additional perturbation potentials neglected in the original diagonalization of the electronic Hamiltonian.

Calculational methods based on this approximation have been of two main types, multistate close-coupling and potential-energy curve-crossing calculations. The former involves the detailed calculation of eigenfunctions, eigenenergies, and transition-matrix elements for all the "important" molecular states. This method has therefore been limited to the treatment of problems where only a relatively small number of states need be considered. To date the multicharged ion-atom problems that have been treated in this manner are $He^{2+}+H$ (Ref. 21), $C^{4+}+He$ and $B^{3+}+He$ (Ref. 22), $C^{4+}+H$ and $B^{3+}+H$ (Ref. 23), and $C^{6+}+H$ (Refs. 24, 25). As will be pointed out below, there are many other cases where the number of important states can be quite large.

Curve-crossing methods and their variants have been used extensively to estimate cross sections.[25-27] Their utility hinges on finding simple approximation procedures for determining the required potential-energy curves and transition-matrix elements. In the case of multicharged-ion–atom electron-capture collisions, the methods of Bates and Moiseiwitch[26] and others[27,28] may be employed to determine approximate potential-energy curves. Here the initial-state potential curve is approximated by a constant term plus an attractive induced-polarization term. The final-state curves are approximated by constant terms plus a Coulomb-repulsion term. Each curve-crossing point R_c is then easily determined, and each transition-matrix element is calculated only at the relevant R_c. These approximate curves and matrix elements are then used in either Landau-Zener,[29] ionic-covalent,[30] or exponential-model[31] calculations and cross sections determined. Estimates based on these methods often ignore interference effects associated with multiple crossings. Transitions induced by the rotation of the internuclear axis are not treated by means of these model approaches.

When a large number of curve crossings exist within a small range of internuclear separation, an "absorbing-sphere approximation"[32,33] may be used to estimate the cross section. The total transition probability is assumed to be unity for impact parameters less than some average crossing distance R_a characteristic of the multiple crossing, and near zero otherwise. The cross section is then simply set equal to πR_a^2. Despite its simplicity, this procedure places reasonable upper bounds on the cross sections.

III. EXPERIMENTAL METHODS AND PROCEDURES

Cross sections in the present work were measured by means of a standard beam–gas-target method. Gas molecules or atoms were dissociated, ionized, and extracted from an ion source. After acceleration by a known potential difference, an ion beam whose charge, mass, and energy were all well known was tightly collimated and allowed to pass through a gas target of well-known composition and thickness. The scattered ions were then analyzed according to charge and energy and finally collected.

The source of the highly charged ions used in the present experiment was the Oak Ridge Penning ion-source test stand.[34,35] This source-accelerator is capable of production and acceleration of ions of practically any element which can be put into a gaseous compound. The accelerating voltage is limited to a ~30-kV maximum by high-voltage breakdown. The ~5-kV mimimum value is limited by ion-optical trajectory considerations. The accelerated ions are deflected by the same static magnetic field used to confine the dc arcs that produce the ion source plasma so that, below about 5 kV, the accelerated ions are deflected too much to be transmitted. For the same reason, H^+ beams are not produced by this source. Until

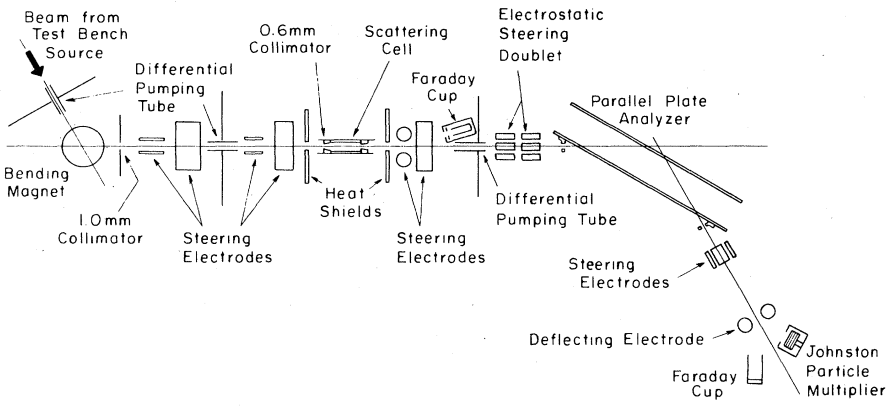

FIG. 1. Schematic of the apparatus used to measure electron-capture cross sections. A beam of ions from the test bench entered from the left, was charge-state analyzed by a 60° magnetic bend, collimated, and allowed to interact with the target. Ions leaving the target were charge-state analyzed in a parallel-plate electrostatic analyzer and detected with a Johnston Laboratories Model MM1 particle multiplier.

recently the only totally stripped ion species successfully extracted from the source and used in experiments have been $^4He^{2+}$ and $^3He^{2+}$. A weak B^{5+} beam was observed by us in 1976, but its magnitude was insufficient for experimentation. The only hydrogenlike ions that have been successfully extracted and used in experiments have been He^+ and B^{4+} and in rare instances C^{5+}. Ions of first-row elements with two or more electrons are routinely available.

A schematic diagram of the experimental apparatus is shown in Fig. 1. Ions with a particular mass-to-charge ratio were delivered by the test-bench source-accelerator and entered the experimental apparatus through a long, small-bore differential pumping tube. All vacuum seals in the experimental apparatus employed metal gaskets, and the base pressure was typically $(1-3)\times 10^{-8}$ Torr. During data acquisition the pressures on either side of a first differential pumping tube were typically $(1-2)\times 10^{-6}$ and 10^{-8} Torr. It was observed that a test-bench pressure of 10^{-4} Torr was required to raise the pressure in the first part of our experimental apparatus to 2×10^{-8} Torr. Immediately after entering our experimental apparatus, the ion beam was reanalyzed magnetically in order to remove lower-charge-state components produced by charge-changing collisions with the background gas in the last meter or so of the test bench. This purified beam was collimated to a beam spot with a diameter at the target of 0.6 mm and with a half-angular divergence of 0.5 mrad. The collimated beam entered the scattering cell where it underwent predominantly single collisions with the target species.

Scattered beams emerging from the cell traveled between various electrostatic steering electrodes and into a large parallel-plate electrostatic analyzer.[36,37] The analyzer dispersed ions with different charges, with a particular charge-state component q' transmitted through its exit aperture when the voltage V_{PPA} on the analyzer was given by

$$V_{PPA} = \alpha(q/q')V_{acc},$$

where q is the charge state of the ions in the incident beam, V_{acc} is the acceleration voltage, and α is a constant depending on the analyzer geometry. For our analyzer α was found experimentally to be equal to 0.4. The charge state of the incident beam was determined simply by taking ratios of the values V_{PPA} needed to transmit various charge-exchange-produced charge states, with other experimental parameters held constant.[20] These ratios must always be ratios of integers; for example, $V_{PPA}(q)/V_{PPA}(q-1) = (q-1)/q$.

After leaving the analyzer, ions traveled between additional steering electrodes and were finally deflected either into a Faraday cup or onto the cathode of a Johnston MM1 particle multiplier. All cross section data were taken with the particle multiplier operating in a pulse counting mode. The pulse-handling electronics system, consisting of unmodified *NIM* modules, is shown schematically in Fig. 2. It was checked experimentally that this circuitry could handle periodic pulse rates as high as 1.5 MHz without pulse loss. During data acquisition, beam-particle average pulse rates were kept below 10 kHz.

Transmission of the ion beam through the parallel-plate analyzer was checked in two ways. The first was a direct one. A relatively intense N^{3+} beam was passed through the gas cell and the ions then deflected into a biased Faraday cup located off axis just past the scattering cell. This ion current was then compared with that measured when the N^{3+} beam was deflected into another off-axis biased Faraday cup located beyond the parallel-plate analyzer. Greater than 95% transmission was observed. Measurements were also made with N^{2+} ions formed by electron-capture collisions of N^{3+} ions in the scattering cell. Greater than 95%

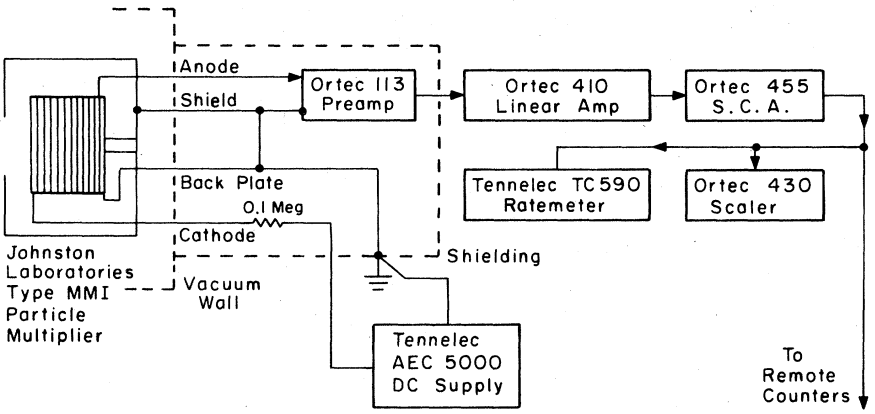

FIG. 2. Particle-multiplier pulse-handling system. Pulses from the particle multiplier were amplified, discriminated, and counted by means of unmodified NIM electronics. This circuit could handle periodic pulse rates as high as 1.5 MHz without pulse loss.

transmission was found for these ions as well. The second transmission check was done by electrostatically scanning a beam across the entrance to the analyzer. Such scans exhibited flat tops for deflections both perpendicular to and in the dispersion plane of the analyzer. Such flat tops are characterisitic of total transmission and collection of the scattered-beam angular distributions. They also indicate that the inverse of the resolution of the analyzer, determined from the geometry to be about 5%, was larger than the fractional energy spread in the ion beam. This is consistent with an earlier measurement which obtained a value of 50–100 eV per unit of charge for the beam energy spread.[35]

The gas-handling system for the target consisted of a stainless-steel reservoir equipped with appropriate gas feed and pumpout valves, a thermocouple gauge tube, and a mechanical pressure gauge. A forepump with copper mesh and liquid-nitrogen-cooled foreline traps was used to evacuate the reservoir to pressures below 10^{-3} Torr. The reservoir leak-up rate with the gas bottles and forepump valved off was below 5×10^{-3} Torr/min. Regulated by a Varian leak valve, the gas flow could be directed either to the scattering cell or bypassed around it into the vacuum system. Thus the data could be corrected for those scattering events produced by gas outside the cell simply by subtracting the signal with the bypass valve open from that with it closed, a well-established experimental technique.[38] All the target gases used were at least 99.99% pure. Considering the relative sizes of the cross sections for the various gases, it is believed that impurity levels as high as 1% would affect the quoted cross section values negligibly, except for certain specific cases. Cross sections were often measured at more than one target density, to verify that multiple-collision effects were negligible ($\leq 2\%$). Larger effects did arise in some two-electron-capture cross section measurements, where signals from two one-electron-capture collisions were $\leq 10\%$ of the two-electron-capture signal. In such cases our results contain appropriate corrections.

Data acquisition procedures are outlined below. A particular ion beam was extracted from the source and tuned through the apparatus. Beam tuning was considered satisfactory when all steering voltages past the scattering cell were reduced to zero, with the exception of the parallel-plate analyzer and the final ion-beam deflector. Under these conditions the collimated beam transmission through the entire apparatus was $\geq 95\%$ because of prior precise optical alignment of the entire apparatus. The reservoir, gas lines, and gas tank regulator were evacuated below 10^{-2} Torr, whereupon the regulator was valved off and a gas bottle opened to charge the regulator. The reservoir and gas lines were evacuated further to below 10^{-3} Torr, whereupon appropriate valves were closed. The reservoir was carefully filled with gas until the mechanical pressure gauge read a particular value, usually 5 psig (about 1000 Torr absolute). The leak valve was opened, with the bypass valve closed, until (1–5)% of the incident ion beam was converted to lower charge states. Measurements were made of the intensities I_q, I_{q-1}, and I_{q-2} of the three main charge-state components of the scattered ion beams by manual scanning of the voltage on the parallel-plate analyzer and recording the output pulse rate of the particle multiplier. The gas bypass valve was opened and the measurements repeated. Several cycles of closed and open bypass valve were done for each ion and gas.

The reservoir was then evacuated as outlined above and filled with a different gas to the same mechanical gauge pressure. The leak valve was not readjusted. For molecular flow conditions the particle density of gas in the scattering cell was independent of gas type for fixed leak-valve setting

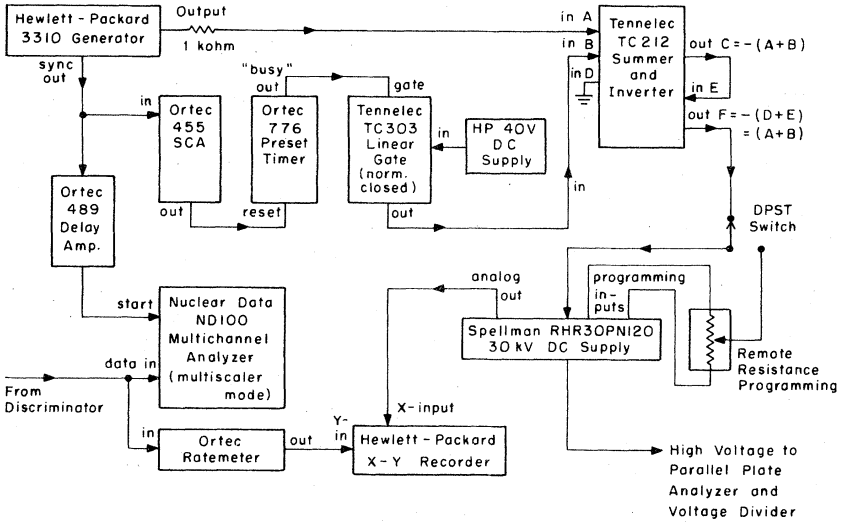

FIG. 3. Parallel-plate analyzer sweep circuitry. A signal generator and standard NIM logic modules produced a three-step waveform to drive a Spellman high-voltage supply acting as an operational amplifier. Each step of the waveform was continuously adjustable in amplitude, and the time durations of the steps were set in the ratios of 1:2:4. In this way the system spent progressively greater time counting the less intense charge-transferred beams.

and fixed absolute reservoir pressure.[14] Hence the target thickness was a constant, independent of gas type, and direct comparisons of relative cross sections for different ions and gases could be made simply by comparing scattering signals. Finally, one could determine the target thickness by measuring a scattering signal for a reaction with a well-known cross section (such as $He^{2+} + Ar \rightarrow He^{+} + Ar^{+}$).

One of the important technical problems associated with these experiments was beam instability. The average intensity of beams emitted by the test-bench source often changed by as much as (10–20)% over a time period of 30 sec, the time needed to make one manual scan of the parallel-plate analyzer. To combat this the sweeping of the parallel-plate analyzer voltage was automated with the circuit shown in Fig. 3. Its output, a staircase waveform consisting of three steps with independently adjustable amplitudes and widths, was used to program the Spellman high-voltage supply which provided the voltage for the parallel-plate analyzer. A pulse synchronized with the beginning of each complete three-step cycle triggered the mutlichannel scaler (MCS) to step sequentially through 256 channels and to reset to channel zero. The dwell time per channel and overall cycle period were adjusted to reset the MCS a small fraction of a second before the end of the three-step cycle. By appropriate adjustment of the step amplitudes the voltage on the parallel-plate analyzer would be made to step from the center of the transmission peak of the incident charge state q to the center of each of two other transmission peaks, usually $q-1$ and $q-2$. Many complete cycles, each of about 12 sec duration, could therefore be taken in order to average out incident-beam-intensity variations.

About 50% of the data presented here was taken by the automated system outlined above. The remaining data were taken manually. No datum taken manually was considered acceptable if the incident-ion count rate had changed by more than 5% from the beginning to the end of an analyzer scan.

A typical cross section $\sigma^{Y}_{q,q-1}(X)$ for ions of atomic species Y with initial charge q incident on gas type X was determined by means of the single-collision regime formula

$$\sigma^{Y}_{q,q-1}(X) = [S^{Y}_{q,q-1}(X)/S^{He}_{21}/Ar)]\sigma^{He}_{21}(Ar),$$

where $S^{Y}_{q,q-1}(X)$ is a charge-capture signal defined below and $He^{2+} + Ar \rightarrow He^{+} + Ar^{+}$ is shown as the normalization reaction. The signal $S^{Y}_{q,q-1}(X)$ is given by

$$S^{Y}_{q,q-1}(X) = \left(\frac{I^{Y}_{q-1}}{I^{Y}_{q}+I^{Y}_{q-1}+I^{Y}_{q-2}}\right)^{in}(X) - \left(\frac{I^{Y}_{q-1}}{I^{Y}_{q}+I^{Y}_{q-1}+I^{Y}_{q-2}}\right)^{dump}(X),$$

where I^{Y}_{j} refers to the intensity of ions of atomic species Y and charge state j entering the particle detector. The superscripts "in" and "dump" refer to gas X entering the cell and bypassed into the vacuum system, respectively.

An additional technical problem was the observation that the test bench did not produce purely dc beams. Although the arcs used to generate the source plasma were presumably dc, the ions generated by the source were sometimes found to come in pulses with repetition rates of 50–100 kHz and "beam-off" to "beam-on" time ratios as large as 50 for some ion species and source conditions. Therefore a low average beam intensity did not ensure that the instantaneous count rate was also

low. Since the particle multiplier and accompanying electronics were nonlinear at high instantaneous count rates, there was concern over possible systematic errors associated with comparing data taken for different ions or different source conditions. Such errors would lead to the observation of artifically high scattering-signal ratios, since the detection efficiency of the high-intensity incident charge state would be lower than the detection efficiency of the low-intensity lower charge states. During an experimental run made subsequent to the collection of much of the data, a systematic study of the beam-pulsing phenomenon led to the conclusion that one could not reliably compare data taken for different incident ion species if the average incident beam intensity were larger than about 2×10^3 sec^{-1}. At higher count rates the beam pulsing could produce systematic errors in cross section values that might be as large as 15% for 10^4 sec^{-1}. By careful adjustment of the source arc conditions one could usually reduce the beam-off to beam-on time to a level undetectable by an oscilloscope monitoring the output of the pulse amplifier. The bulk of the data (here called "early" data) had, however, been taken with incident-ion count rates around 10^4 sec^{-1}. Thus it was decided that our early data should be used only for cross section comparisons from one target species to another, since scattered beam intensities were more than an order of magnitude smaller than incident beam intensities, which differed little from one target gas to another. For data taken with incident-ion count rates below 2 kHz, one could compare different ion species as well as different targets.

IV. DATA NORMALIZATION PROCEDURES

A measurement was made of the scattering signal for incident $^3He^{2+}$ ions with an energy of 16 keV producing $^3He^+$ after scattering in an Ar gas target. The cross section for this He^{2+} process has been measured independently by Shah and Gilbody[13] and by Bayfield and Khayrallah,[14] who fould it equal to (9.8 ± 1.0) and $(9.3\pm1.1)\times10^{-16}$ cm^2, respectively. Measurements were then made of the scattering signals for incident B^{4+} and C^{4+}, both at energies of 32 keV, producing B^{3+} and C^{3+}, respectively, when incident on the same Ar target. The cross sections σ^B_{43}(Ar) and σ^C_{43}(Ar) were thus normalized to σ^{He}_{21}(Ar). This procedure was followed with full knowledge and monitoring of the beam-pulsing problem. Incident-ion-beam average intensities were kept below 10^3 sec^{-1}, and no beam pulsing could be discerned. The cross section σ^C_{43}(Ar) determined in this way was found to be equal to that reported by Crandall.[39] Cross sections for the other target gases H_2 and He were determined from cross section ratios H_2 to Ar and He to Ar calculated by means of early data. The cross sections σ^B_{43}(He), $\sigma^B_{43}(H_2)$, σ^C_{43}(He), and $\sigma^C_{43}(H_2)$ were therefore determined for the single incident-ion energy of 32 keV. The cross section $\sigma^C_{43}(H_2)$ was found to be in close agreement with the measurement of Crandall *et al.*[18]

The remaining cross sections for C, N, and O ions with charge $q>2$ incident on He and Ar were determined by direct normalization to corresponding values for H_2 given in Ref. 18. Besides our present measured values of $\sigma^C_{43}(H_2)$ there are additional measurements indicating that the cross sections determined by Crandall *et al.*[18] for H_2 targets are accurate to within about $\pm10\%$.[40]

The cross sections for C^{2+}, N^{2+}, and O^{2+} incident on Ar, H_2, and He were normalized by comparing each 2+-incident-ion scattering signal to *all* the scattering signals at the same nominal target thickness for the various previously listed ions incident on H_2. Residual effects ($\lesssim15\%$) associated with undetermined beam pulsing thus persist in these data. The quoted errors for each of these 2+ cross sections were enlarged to account for the possible remaining systematic error. Our value of 10.2 ± 2.8 Å^2 for $\sigma^C_{21}(H_2)$ at 16 keV compares well with that of Nutt *et al.* of 9.2 ± 0.6 Å^2 at 14 keV.[44]

The cross sections for B^{3+} and B^{2+} incident on Ar at 24 and 16 keV, respectively, were determined by a normalization to the cross section for B^{4+} incident on Ar at 32 keV as determined above. These comparisons were done at "low" count rates where beam pulsing effects were negligible. The cross sections for B^{3+} and B^{2+} on H_2 and He were determined by normalization to the respective values determined for an Ar target. The data for the various boron ions at energies other than $8q$ keV were normalized to the cross sections for the respective ions at $8q$ keV incident on Ar.

The various double-electron-capture cross sections were normalized to single-capture cross sections measured simultaneously for the same incident-ion species, ion beam intensity, and target gas. Thus σ^B_{31}(Ar) is normalized to σ^B_{32}(Ar), $\sigma^C_{42}(H_2)$ to $\sigma^C_{43}(H_2)$, etc.

Estimates of the errors in a typical quoted cross section value are tabulated according to source in Table I. The total error was obtained by combining the individual errors in quadrature.

V. RESULTS AND DISCUSSION

The cross sections for boron ions incident on Ar, H_2, and He are shown in Fig. 4, 5, and 6,

TABLE I. Sources of error and their maximum magnitudes.

Single-electron-capture cross sections (±%)
(i) Absolute cross section scale: 15%
(ii) Statistical uncertainty of cross section ratios: 10%
(iii) Possible beam-pulsing systematic effects: 15% for the 2+ ions (except boron) and 5% for all other ions
(iv) Impurity of target gases: 0.1%
(v) Incomplete collection of scattered ion angular distributions: 5%

TABLE II. Energy defects and initial-state–final-state crossing distances for capture into various states in the collision systems $B^{q+}+Ar$, $B^{q+}+H_2$, and $B^{q+}+He$ for $q=2,3$, and 4. Crossing distances were estimated using the methods of Bates and Moiseiwitsch (Ref. 26). Dipole polarizabilities were taken to be 1.4 a.u. for He and 11 a.u. for Ar (Ref. 46). The polarizability of H_2 was taken to be 6.94 and 4.82 a.u. for ion-molecule separation vectors parallel to and perpendicular to, respectively, the molecular internuclear axis (Ref. 51).

Final ionic state	Helium		Argon		Molecular hydrogen	
	ΔE	R_c	ΔE	R_c	ΔE	R_c
			$B^{2+}(1s^2 2s\ ^2S)$ incident			
$B^+(1s^2 2s^2\ ^1S)$	0.6	4.5	9.4	4.3	9.7	3.8–4.0
$B^+(1s^2 2s 2p\ ^3P)$	−4.1		4.8	6.5	5.1	5.9–6.0
$B^+(1s^2 2s 2p\ ^1P)$	−8.5		0.3	91	0.6	45
$B^+(1s^2 2p^2\ ^3P)$			−2.9		−2.6	
			$B^{3+}(1s^2\ ^1S)$ incident			
$B^{2+}(1s^2 2s\ ^2S)$	13.3	4.4	22.2	4.1	22.5	3.6–3.8
$B^{2+}(1s^2 2p\ ^2P)$	7.3	7.6	16.2	4.8	16.5	4.3–4.5
$B^{2+}(1s^2 2s\ ^2S)$			8.7[a]	7.1		
$B^{2+}(1s^2 2p\ ^2P)$			2.7[a]	20		
$B^{2+}(1s^2 3s\ ^2S)$			−0.2		0.1	54
$B^+(1s^2 2s^2\ ^1S)$	−16		20	4.3	32	3.0–3.3
$B^+(1s^2 2s 2p\ ^3P)$			15	5.0	27	3.3–3.5
$B^+(1s^2 2s 2p\ ^1P)$			11	6.0	22	3.6–3.8
$B^+(1s^2 2s 3s\ ^3S)$			3	18	14	4.7–4.9
$B^+(1s^2 2s 3s\ ^1S)$			2	30	14	
$B^+(1s^2 2s 3p\ ^3P)$			2	27	14	
$B^+(1s^2 2s 3p\ ^1P)$			2		14	
$B^+(1s^2 2p^2\ ^3P)$			1.4	39	13	4.9–5.1
$B^+(1s^2 2p^2\ ^3D)$			1.0	54	13	
$B^+(1s^2 2p^2\ ^1D)$			0.5	110	12	5.2–5.4
$B^+(1s^2 2s 4s\ ^3S)$			−0.9		11	5.6–5.7
$B^+(1s^2 2s 4s\ ^1S)$					11	
$B^+(1s^2 2s 4p\ ^3P)$					10	6.0–6.2
$B^+(1s^2 2s 4d\ ^3D)$					10	
$B^+(1s^2 2p^2\ ^1S)$					9.6	6.2–6.4
			$B^{4+}(1s\ ^2S)$ incident			
$B^{3+}(1s^2\ ^1S)$	235	1.3	244	2.2	244	1.8–2.0
$B^{3+}(1s 2s\ ^3S)$	36	2.9	45	3.8	45	3.2–3.5
$B^{3+}(1s 2s\ ^1S)$	32	3.1	41	3.9	41	3.4–3.6
$B^{3+}(1s 2p\ ^3P)$	32		41		41	
$B^{3+}(1s 2p\ ^1P)$	30	3.3	38	4.0	38	3.5–3.7
$B^{3+}(1s 3s\ ^3S)$	1.4	58	10	8.8	10	8.5–8.6
$B^{3+}(1s 3s\ ^1S)$	0.2	410	9	9.6	9	9.4–9.5
$B^{3+}(1s 3p\ ^3P)$	0.2		9		9	
$B^{3+}(1s 3p\ ^1P)$	−0.6		8	11	8	10.4–10.5
$B^{3+}(1s 3d\ ^3D)$	−0.4		8		9	

TABLE II. (*Continued*)

Final ionic state	Helium		Argon		Molecular hydrogen	
	ΔE	R_c	ΔE	R_c	ΔE	R_c
$B^{3+}(1s3d\,^1D)$	−0.4		8		9	
$B^{3+}(1s4s\,^3S)$	−10		−1		−1	
$B^{2+}(1s^22s\,^2S)$	218	1.4	254	2.2	266	1.8–1.9
$B^{2+}(1s2s^2\,^2S)$	18	6.2	54	3.7	66	2.9–3.1
$B^{2+}(1s2p(^3P)2s)$	15	7.4	51	3.8	63	3.0–3.2
$B^{2+}(1s2s(^3S)2p)$	14	7.9	49	3.9	61	3.0–3.3
$B^{2+}(1s2p(^1P)2s)$	13	8.5	48	3.9	60	3.1–3.3
$B^{2+}(1s2s(^1S)2p)$	10	11	45	4.0	57	3.1–3.3
$B^{2+}(1s2s(^3S)3s)$	−2.6		33	4.7	45	3.5–3.7
$B^{2+}(1s2s(^1S)3s)$	−6.8		29	5.0	41	3.7–3.9
$B^{2+}(1s2s(^3S)3p)$	−4.2		31	4.8	43	3.6–3.8
$B^{2+}(1s3s^2\,^2S)$	−37		−1		10	11.0–11.1
$B^{3+}(1s^2\,^1S)$			230[a]	2.2		
$B^{3+}(1s2s\,^3S)$			32[a]	4.3		
$B^{3+}(1s2s\,^1S)$			27[a]	4.7		
$B^{3+}(1s2p\,^3P)$			27[a]			
$B^{3+}(1s2p\,^1P)$			25[a]	4.9		
$B^{3+}(1s3s\,^3S)$			−3[a]			

[a] The final Ar^+ ion left in its first excited state.

respectively. Except for B^{2+} + He, the data show little dependence on the collision energy in this range. The lack of a monotonic dependence of the cross sections on incident-ion charge q is displayed by the opposite q ordering of the cross sections for He compared to those for Ar and H_2. It may be further noted that the cross sections for H_2 and Ar are strikingly similar, the ones for H_2 being uniformly lower than those for Ar by about 20%.

The energy defects for certain final-state channels for the various collision partners are presented in Table II.[49] Binding energies of the various boron-ion states were taken from Eidelsburg[41] for the B^{4+} case and from Moore[42] for the B^{2+} and B^{3+} cases. The B^{2+} + He collision is almost resonant for capture into the ground state, but the B^{2+} + Ar and B^{2+} + H_2 collisions each have three exothermic final states. The methods of Bates and Moiseiwitsch[26] can be used to calculate final-state crossing points with the initial state, which for B^{2+} + Ar occur at internuclear separations of 4, 6.5, and 90 a.u., respectively. For the collision velocities here, it is expected that the two inner crossings are the important ones.

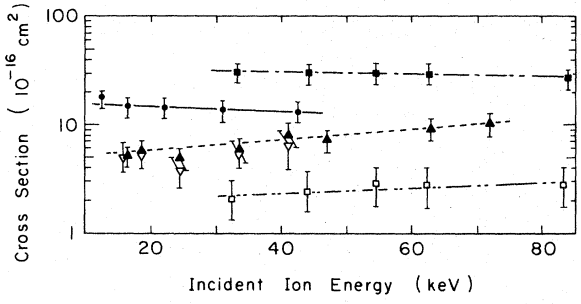

FIG. 4. Electron-capture cross sections for boron ions in argon. Solid data points are σ_{43} (squares), σ_{32} (triangles), and σ_{21} (dots); open data points are σ_{42} (squares) and σ_{31} (triangles). The cross sections clearly show little dependence on the collision energy. Furthermore, the single-capture cross sections do not increase monotonically with increasing initial charge state. Note that $\sigma_{31} \simeq 0.8\,\sigma_{32}$, indicating that multiple-electron effects are important.

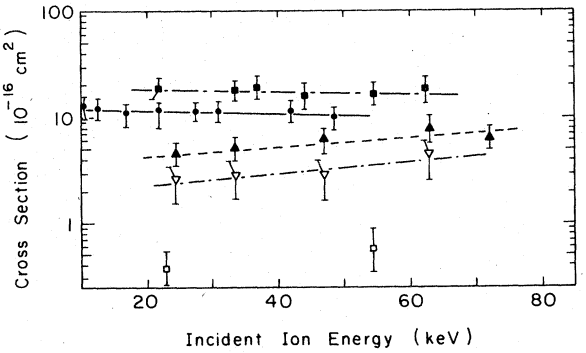

FIG. 5. Electron-capture cross sections for boron ions in molecular hydrogen. Symbols for data points as in Fig. 4. Note that these data closely parallel those for argon.

TABLE III. Survey data for various ions in Ar and He. Listed also for comparison are cross section values from other experiments (not necessarily done at exactly the same collision energy).

Reaction	Present data	Cross section ($\times 10^{-16}$ cm^2) Crandall *et al.*[a]	Zwally *et al.*[b]	Goldhar *et al.*[c]	Nutt *et al.*[d]	Hasted and Smith[e]
B^{2+} + He	0.28 ± 0.06 16 keV					
H_2	13.8 ± 2.8					
Ar	16.2 ± 3.6					
B^{3+} + He	7.2 ± 2.5 24 keV	12 ± 2[f] 24 keV	14 ± 1[g] 24 keV			
H_2	4.5 ± 1.0					
Ar	4.9 ± 1.1					
B^{4+} + He	4.0 ± 1.2 32 keV					
H_2	19.6 ± 5.9					
Ar	30 ± 8					
C^{2+} + He	3.2 ± 0.9 16 keV		3.2 ± ?[h] 16 keV			4 5 keV
H_2	10.2 ± 2.8				9.21 ± 0.61 14 keV	
Ar	7.5 ± 2.1		8.4 ± ?[h] 16 keV			20 5 keV
C^{3+} + He	14.1 ± 4.0 24 keV			14, E = ?		
Ar	7.3 ± 1.8			10, E = ?		
C^{4+} + He	1.87 ± 0.55 32 keV	2.9 ± 0.4[f] 32 keV	7 ± 1[j] 32 keV	1, E = ?		
H_2	23 ± 5	25 ± 4[i] 32 keV				
Ar	28 ± 6	28 ± 4[f] 32 keV	90 ± 20[j] 32 keV	56, E = ?		
N^{2+} + He	5.3 ± 1.5 16 keV					7 5 keV
H_2	3.1 ± 1.0					
Ar	5.5 ± 1.8					19 5 keV
N^{3+} + He	4.6 ± 1.7 24 keV					
Ar	9.0 ± 1.8					
N^{4+} + He	1.5 ± 0.6 32 keV					
Ar	31 ± 11					
N^{5+} + He	10.6 ± 3.5 40 keV	11.1 ± 1.6[f] 40.5 keV				
Ar	26 ± 5					
O^{2+} + He	6.2 ± 1.7 16 keV					
H_2	1.6 ± 0.4					
Ar	4.0 ± 1.1					
O^{3+} + He	2.6 ± 0.5 24 keV	3.7 ± 0.6[k] 25.8 keV				
Ar	14.8 ± 3.0					
O^{4+} + He	7.9 ± 1.8 32 keV					
Ar	31 ± 6					

TABLE III. (*Continued*)

Reaction	Present data	Crandall *et al.*[a]	Cross section ($\times 10^{-16}$ cm^2) Zwally *et al.*[b]	Goldhar *et al.*[c]	Nutt *et al.*[d]	Hasted and Smith[e]
O^{5+} + He	17.5 ± 6.0 40 keV					
Ar	26 ± 7					
O^{6+} + He	10.4 ± 2.8 48 keV	11.8 ± 1.8[f] 49.2 keV				
Ar	50 ±14					

[a] References 18, 19, and 48.
[b] References 15, 16, and 45.
[c] Reference 47.
[d] Reference 44.
[e] Reference 10.
[f] Reference 19.
[g] Reference 16.
[h] Reference 45.
[i] Reference 18.
[j] References 15 and 45.
[k] Reference 48.

Since many possible exothermic final states are possible for the B^{4+} collision processes, for these cases there are probably a large number of important curve crossings. In particular, those leading to a captured electron in the $n = 3$ states of B^{3+} should be most important for H_2 and Ar. These are expected to have crossings in the vicinity of $9a_0$. For He, the $n = 3$ states of B^{3+} have crossings at internuclear separations in excess of $50a_0$. Since the relative velocity of the colliding particles is also fairly large ($v \simeq 0.3$ a.u.), one expects little contribution to the cross section from these far crossings. Therefore the cross section is most likely determined by the crossing with $n = 2$ states of B^{3+}, which occur at around $3a_0$. One should note that multielectron processes such as

$$B^{4+} + He \rightarrow B^{3+}(1s^2) + He^{2+} + e^-,$$

$$B^{4+} + Ar \rightarrow B^{3+}(1s^2) + Ar^{3+} + 2e^-, \text{ etc.}$$

are also exothermic and contribute to the apparent single-capture cross sections. Kishenevskii and Parilis[43] have performed calculations for such Auger ionization processes as the first reaction listed above. With estimated cross sections of order 10^{-16}–10^{-15} cm^2, they can be an important contribution to the overall measured cross sections.

With a much smaller number of exothermic channels, the B^{3+} + Ar problem is much simpler than the corresponding B^{4+} problem. The double-electron-capture states $B^+(1s^22s^2)$ and $B^+(1s^22p2s)$ are important final channels and have crossings with the initial state at distances comparable to the single-capture $B^{2+}(1s^22s)$ and $B^{2+}(1s^22p)$ final states. The experimental consequences are that σ_{31}(Ar) is only ~20% lower then σ_{32}(Ar) throughout

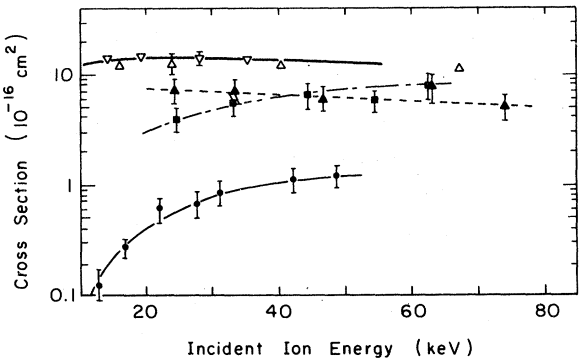

FIG. 6. *Electron-capture cross sections for boron ions in helium.* Present data are the solid points labeled as in Fig. 4. Values of σ_{32} from other work are △ Crandall (Ref. 19) and ▽ Zwally and Cable (Ref. 16). The heavy solid curve is the theoretical result of Shipsey *et al*. (Ref. 22).

the energy range investigated.

The B^{3+} + He collision is probably the simplest electron-capture process in the present experimental study. From a curve-crossing point of view, there are only two important, well-separated crossings. According to a close-coupling calculation for this problem in the present energy range,[22] capture takes place predominantly into the $B^{2+}(1s^2 2s)$ ground state; less than 10% goes into the $B^{2+}(1s^2 2p)$ excited state. The results of this calculation are shown with the data in Fig. 6.

The present B^{3+} + He data are somewhat lower than the results of two previous measurements[16,19] but are not inconsistent with them when (nonstatistical) 90%-confidence error bars of all the measurements are considered. The differences in these measurements are discussed further below.

Our survey results for the ions $C^{2,3,4+}$, $N^{2,3,4,5+}$, and $O^{2,3,4,5,6+}$ incident on Ar, He, and, in some cases, H_2 are presented in Table III together with values for some of these cross sections measured by other workers. Since the present data were taken at a fixed acceleration potential of 8 kV, the velocities of the incident ions, which scale with the square root of the charge-to-mass ratio, range from 4.4×10^7 cm/sec for O^{2+} to 7.6×10^7 cm/sec for the most energetic ion, O^{6+}. As was the case with boron, there is no monotonic variation of the cross sections with incident charge for fixed target species. However, a gross trend toward larger cross sections for larger incident charge is apparent.

The present results compare well with those of other investigators. There is, for example, good agreement with a very slight energy extrapolation of the results of Nutt *et al.*,[44] for $C^{2+} + H_2$. There is also good agreement with the results of Zwally[45] for C^{2+} + Ar and C^{2+} + He. However, the results of Zwally and Koopman[15] for C^{4+} + He and C^{4+} + Ar are in marked disagreement with the present results, which are consistent with those of Crandall.[19] The C^{4+} data of Zwally[45] and Zwally and Koopman[15] were taken by means of an instantaneously intense pulsed ion source. Low-intensity continuous beams of several ion species including C^{2+} were used in a rather special particle-detector calibration procedure[45] that was then extrapolated to C^{4+} and C^{3+} ions. The agreement between Zwally's C^{2+} data and the present C^{2+} data thus suggests that the extrapolation of the calibration procedure to C^{4+} and C^{3+} was in some way inaccurate.

The present cross sections for C^{4+}, N^{5+}, O^{3+}, and O^{6+} (as well as B^{3+}) ions colliding with helium atoms agree with those of Crandall[19] when 90%-confidence error bars are considered. The present values, however, are always lower than those of Ref. 19 for these collision systems. In the present experiment, data were taken for each incident ion beam for the three target gases He, Ar, and H_2 in rapid succession. Thus the present experimental cross section ratios for fixed incident-ion species but different target species are determined more accurately than the individual cross sections themselves. Such ratios of cross sections for a He target to those for a H_2 target for the ions B^{3+}, C^{4+}, N^{5+}, O^{3+}, and O^{6+} are listed in Table IV along with similar ratios calculated with the results of Crandall *et al.*[18] and Crandall.[19] The errors quoted for cross section ratios were determined for these data by combining the individual errors in quadrature. The ratios determined from the present data are systematically smaller than those determined from Refs. 18 and 19, although in every case there is agreement of varying degrees when all experimental errors are considered. When ratios of the cross section ratios are calculated and averaged, one obtains the number 1.26 for the ratios of Crandall divided by present ratios, with a standard deviation of 0.17. This suggests that there may be a real systematic shift between the two sets of data.

VI. SUMMARY

Cross sections for single-electron capture by multiply charged boron ions incident on Ar, H_2,

TABLE IV. Comparison of cross section ratios for He and H_2 targets.

Incident ion	$\sigma_{q,q-1}(\mathrm{He})/\sigma_{q,q-1}(H_2)$ Present data	References 18 and 19	Column 3/column 2
B^{3+}	1.60 ± 0.24	2.00 ± 0.41 [a]	1.25
C^{4+}	0.081 ± 0.012	0.116 ± 0.024	1.43
N^{5+}	0.50 ± 0.07	0.52 ± 0.11	1.05
O^{3+}	0.27 ± 0.04	0.39 ± 0.08	1.44
O^{6+}	0.29 ± 0.04	0.33 ± 0.07	1.14
			Average= 1.26
			Standard deviation= 0.17

[a] This ratio was determined with a value for $\sigma_{32}^{B}(H_2)$ and its error determined from Ref. 40.

and He at keV energies have been determined experimentally. Also measured were double-capture cross sections for B^{3+} incident on Ar and H_2 and for B^{4+} incident on Ar, H_2, and He. The cross sections for these processes can be understood qualitatively by means of a molecular potential-energy curve-crossing model of the collisions. Double-electron-capture cross sections are often a sizeable fraction of those for single-electron capture.

Single-capture cross sections were also determined for C^{q+} $(2 \leq q \leq 4)$, N^{q+} $(2 \leq q \leq 5)$, and O^{q+} $(2 \leq q \leq 6)$ incident on Ar and He. These data were taken at collision energies of $8q$ keV. In general only an overall tendency toward larger cross sections for larger incident-ion charge is found. The cross sections are found not to depend monotonically on the incident charge.

In cases previously studied by other investigators, agreement within errors is generally found. An exception, that the present results for B^{3+} + He are significantly lower than those of earlier work suggests the existence of a few inconsistencies in the existing data bank of multiply-charged-ion electron-capture cross sections.

ACKNOWLEDGMENT

The work of one of us (J.E.B.) was supported by the Division of Chemical Sciences of the Department of Energy.

---

*Present address: Harvard Center for Astrophysics, 60 Garden Street, Cambridge, Mass. 02138.
†Present address: Dept. of Physics and Astronomy, Univ. of Pittsburgh, Pittsburgh, Pa. 15260.
‡Present address: Dept. of Physics, Univ. of Connecticut, Storrs, Conn. 06268.
§Present address: Dept. of Physics, Michigan State Univ., East Lansing, Mich. 48823.

[1]H. Schiff, Can. J. Phys. 32, 3931 (1954).
[2]C. F. Barnett, in *The Physics of Electronic and Atomic Collisions*, edited by J. S. Risley and R. Geballe (University of Washington, Seattle, Wash., 1976), p. 846.
[3]E. Hinov, Phys. Rev. A 14, 1533 (1976).
[4]A. V. Vinogradov and I. I. Sobelman, Zh. Eksp. Teor. Fiz. 63, 1919 (1972) [Sov. Phys. JETP 36, 1115 (1973)].
[5]W. H. Louisell, M. O. Scully, and W. B. McKnight, Phys. Rev. A 11, 989 (1975); J. F. Seely and W. B. McKnight, J. Appl. Phys. 48, 3691 (1977).
[6]D. L. Jassby, Nucl. Fusion 17, 309 (1977).
[7]D. H. Crandall, in *Proceedings of the Fourth Conference on Scientific and Industrial Applications of Small Accelerators*, edited by J. L. Duggan and J. A. Martin (North Texas State University, Denton, Tex. 1977), p. 157.
[8]G. B. Field, in *Atomic and Molecular Physics and the Interstellar Matter*, edited by R. Balian, R. Encrenaz, and J. Lequeax (North-Holland, Amsterdam, 1975), p. 467.
[9]G. Steigman, Astrophys. J. Lett. 195, L39 (1975); Astrophys. J. 199, 336 (1975); 119, 642 (1975).
[10]J. B. Hasted and R. A. Smith, Proc. R. Soc. A 235, 354 (1956).
[11]See, for example, J. B. Hasted and A.Y. J. Chong, Proc. Phys. Soc. 80, 441 (1962); J. B. Hasted and J. Hussain, *ibid.* 83, 911 (1964); J. B. Hasted, S. M. Igbal, and M. M. Yousaf, J. Phys. B 4, 343 (1971).
[12]W. L. Fite, A. C. H. Smith, and R. F. Stebbings, Proc. R. Soc. A 268, 527 (1968).
[13]M. B. Shah and H. B. Gilbody, J. Phys. B 7, 636 (1974).
[14]J. E. Bayfield and G. A. Khayrallah, Phys. Rev. A 11, 920 (1975).
[15]H. J. Zwally and D. W. Koopman, Phys. Rev. A 2, 1851 (1970).
[16]H. J. Zwally and P. G. Cable, Phys. Rev. A 4, 2301 (1971).
[17]H. Klinger, A. Muller, and E. Salzborn, J. Phys. B 8, 230 (1975).
[18]D. H. Crandall, M. L. Mallory, and D. C.Kocher, Phys. Rev. A 15, 61 (1977).
[19]D. H. Crandall, Phys. Rev. A 16, 958 (1977).
[20]V. V. Afrosimov, A. A. Basalev, G. A. Leiko, and M. N. Panov, in *Proceedings of the Ninth International Conference on the Physics of Electron and Atomic Collisions, City*, 1977 (Publisher, City, 1978), Vol. I, p. 528.
[21]R. D. Piacentini and A. Sallin, J. Phys. B 7, 1666 (1974).
[22]E. J. Shipsey, J. C. Brown, and R. E. Olson, Phys. Rev. A 15, 2116 (1977).
[23]R. E. Olson, E. J. Shipsey, and J. C. Brown, J. Phys. B (to be published).
[24]A. Salop and R. E. Olson, Phys. Rev. A 16, 1811 (1977).
[25]J. Vaaben and J. S. Briggs, J. Phys. B 10, L521 (1977).
[26]D. R. Bates and B. L. Moiseiwitsch, Proc. Phys. Soc. 67, 57 (1954).
[27]T. J. M. Boyd and B. L. Moiseiwitsch, Proc. Phys. Soc. 70, 45 (1957).
[28]A. Dalgarno, Proc. Phys. Soc. A 67, 1010 (1954).
[29]L. D. Landau, J. Phys. (Moscow) 2, 46 (1932); C. Zener, Proc. R. Soc. A 137, 696 (1932).
[30]A. D. Bandrauk, Mol. Phys. 24, 661 (1972); see also M. S. Child, *ibid.* 20, 121 (1971).
[31]J. E. Bayfield, E. E. Nikitin, and A. I. Reznikov, Chem. Phys. Lett. 19, 471 (1973).
[32]R. K. Cacak, Q. C. Kessel, and M. E. Rudd, Phys. Rev. A 2, 1327 (1970).
[33]R. E. Olson and A. Salop, Phys. Rev. A 14, 579 (1976).
[34]M. L. Mallory and E. D. Hudson, IEEE Trans. Nucl. Sci. NS-22, 1669 (1975).
[35]M. L. Mallory and D. H. Crandall, IEEE Trans. Nucl. Sci. NS-23, 1069 (1975).
[36]T. S. Green and G. A. Proca, Rev. Sci. Instrum. 41, 1409 (1970).

[37]G. A. Harrower, Rev. Sci. Instrum. 26, 850 (1955).
[38]J. E. Bayfield, Rev. Sci. Instrum. 40, 869 (1969).
[39]D. H. Crandall (private communication).
[40]R. Phaneuf, F. Meyer, and D. H. Crandall (private communication).
[41]M. Eidelsburg, J. Phys. B 7, 1476 (1974).
[42]C. E. Moore, *Atomic Energy Levels*, Nat. Bur. Stand. U. S. Circ. (U.S. GPO, Washington, D. C., 1949), p. 467.
[43]L. M. Kishenevskii and E. S. Parilis, Sov. Phys. JETP 28, 1020 (1969).
[44]W. L. Nutt, R. W. McCullough, and H. B. Gilbody, J. Phys. B 11, L181 (1978).
[45]H. J. Zwally, University of Maryland Institute for Fluid Dynamics and Applied Mathematics Technical Note BN-582, 1968 (unpublished).
[46]R. R. Teachout and R. T. Pack, At. Data 3, 195 (1971).
[47]J. Goldhar, R. Mariella, and A. Javan, Appl. Phys. Lett. 29, 96 (1976).
[48]D. H. Crandall (private communication).
[49]L. D. Gardner, Ph.D. thesis, Yale University, 1978 (unpublished).
[50]N. J. Bridge and A. D. Buckingham, Proc. R. Soc. A 295, 334 (1966).